Pergamon

Natural variations of Se isotopic composition determined by hydride generation multiple collector inductively coupled plasma mass spectrometry

OLIVIER ROUXEL,[1,]* JOHN LUDDEN,[1] JEAN CARIGNAN,[1] LUC MARIN[1] and YVES FOUQUET[2]

[1]CRPG-CNRS, 15 rue Notre Dame des Pauvres, 54501 Vandoeuvre les Nancy, France
[2]IFREMER DRO/GM, BP 70 29280 Plouzané, France

Abstract—Multiple-collector inductively coupled plasma mass spectrometry has been used for the precise measurement of the isotopic composition of Se in geological samples. Se is chemically purified before analysis by using cotton impregnated with thioglycollic acid. This preconcentration step is required for the removal of matrix-interfering elements for hydride generation, such as transitional metals, and also for the quantitative separation of other hydride-forming elements, such as Ge, Sb, and As. The analyte is introduced in the plasma torch with a continuous-flow hydride generation system. Instrumental mass fractionation is corrected with a "standard-sample bracketing" approach. By use of this new technique, the minimum Se required per analysis is lowered to 10 ng, which is one order of magnitude less than the amount needed for the N-TIMS technique. The estimated external precision calculated for the $^{82}Se/^{76}Se$ isotope ratio is 0.25‰ (2σ), and the data are reported as delta notation (‰) relative to our internal standard (MERCK elemental standard solution). Measurements of Se isotopes are presented for samples of standard solutions and geological reference materials, such as silicate rocks, soils, and sediments. The Se isotopic composition of selected terrestrial and extraterrestrial materials are also presented. An overall Se isotope variation of 8‰ has been observed, suggesting that Se isotopes fractionate readily and are extremely useful tracers of natural processes. *Copyright © 2002 Elsevier Science Ltd*

1. INTRODUCTION

Trace and ultratrace determination of selenium species in environmental and biologic samples has become of increasing interest as a result of its essentialness to life and also because of toxic character of selenium (Frankenberger and Benson, 1994). Chemically similar to sulfur, Se occurs as +6, +4, 0, and −2 valences in a variety of organic compounds and geological settings. Because of the large number of selenium isotopes (six) with a total percentage mass difference between ^{76}Se and ^{82}Se of 7%, in addition to the numerous microbial or abiotic redox transformations, Se isotopes are potentially excellent tracers of geological and biologic processes. Se isotope ratios were first determined by gas-source mass spectrometry (Krouse and Thode, 1962) and more recently by N-TIMS (Johnson et al., 1999) by use of a double spike technique. These results, which included laboratory-simulated fractionation, show that the $^{82}Se/^{76}Se$ ratios vary by as much as 15‰ and indicate that inorganic reduction of soluble oxyanions (Rees and Thode, 1966; Rashid and Krouse, 1985; Johnson et al., 1999) as well as biologic reduction of selenium (Rashid et al., 1978; Herbel et al., 2000) are the dominant cause of Se isotope fractionation.

Within the past 5 yr, scientists have successfully used multiple-collector inductively coupled plasma mass spectrometry (MC-ICP-MS) for the precise isotope measurement of elements with high first-ionization potential such as Hf and W (Halliday et al., 1995). More recently, several studies have been carried out on lighter elements such as Cu, Fe, and Zn (Maréchal et al., 1999; Belshaw et al., 2000; Zhu et al., 2000). For elements such

as Se, near mass 80, which suffer the presence of argide molecular interferences, the development of a hexapole collision cell (Turner et al., 1998) allowing the removal of these isobaric interferences opened new possibilities for the study of this element. Because Se concentration in the Earth's crust and hydrological systems is generally below 0.5 $\mu g/g$ and 0.1 ng/g, respectively, a new, sensitive method has been developed for the precise determination of Se isotopes at the nanogram level. This new technique uses a continuous flow hydride generator coupled to a Micromass MC-ICP-MS and combines the following: (1) the classic and easy-to-operate gas source mass spectrometry technique with instrumental mass fractionation corrected by use of a "standard-sample bracketing" approach; (2) high sensitivity and potential matrix-free effect by use of gaseous hydride introduction in the plasma torch; and (3) precise and accurate isotope ratio measurement by the magnetic sector and multiple collector array of the MC-ICP-MS.

2. MATERIALS AND METHODS

2.1. Sample Preparation

2.1.1. Reagents

We purified 18 $M\Omega$–grade water with a Millipore deionizing system. Distilled nitric and hydrochloric acid were used for the chemical separation and hydride generation (HG). All glassware and Teflon materials were cleaned with concentrated analytical reagent grade nitric acid and distilled water before use. Sodium borohydride solution at 1% was prepared daily after filtration and was stabilized in 0.05% NaOH (analytical grade). Standard Se solution MERCK was obtained from MERCK S.A. Titrisol solution (SeO_2 in HNO_3). Thiol cotton fiber (TCF) used for Se enrichment is prepared via the following procedure described by Yu et al. (1983) and Marin et al. (2001). Thioglycollic acid (62.6 mL), acetic anhydride (34.7 mL), acetic acid (16.5 mL), and concentrated sulfuric acid (0.137 mL) were put in a Teflon beaker and mixed well, and 10 g of medical-grade hydrophile cotton was intro-

* Author to whom correspondence should be addressed (rouxel@crpg.cnrs-nancy.fr).
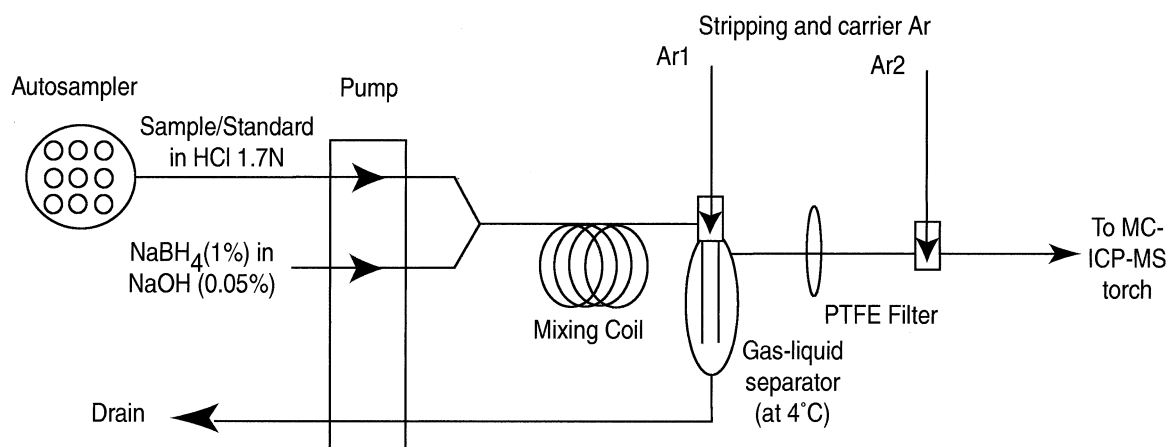
Fig. 1. Schematic diagram of the continuous-flow hydride generator.

duced. The beaker was closed and left for 4 d in water bath at 40°C. The beaker was agitated every day. The TCF was filtered with a sintered-glass funnel and washed with water. The TCF was dried at room temperature for 2 d in a clean box.

2.1.2. Sample decomposition

Silicate rock samples were digested in concentrated HF (10 mL) HNO_3 (5 mL) $HClO_4$ (1 mL) in 60-mL polytetrafluoroethylene (PTFE) digestion bomb. Before sealing, the PTFE containers containing sulfide-rich or carbonate-rich materials were left at room temperature until completely degassed. For organic rich material (e.g., soil and shale), 10 mL of HNO_3 + 1 mL H_2O_2 was first added and taken to incipient dryness. Sealed PTFE containers were left overnight on a hot plate at 120°C and then taken to incipient dryness at 70°C on a hot plate. Sulfide samples were digested in open vessels with 5 mL of HNO_3 and 0.5 mL of $HClO_4$ and were taken to incipient dryness at 60°C on a hot plate. Se loss during digestion has to be avoided by using a HCl-free chemical attack and maintaining the temperature of evaporation below 80°C. The residue obtained after chemical treatment was dissolved in 10 mL of HCl 4 N, and the solution was heated 20 min in a closed vessel in a boiling water. However, longer digestions (60 min) or stronger HCl (6 N) may be necessary to convert all selenate into selenite (Brimmer et al., 1987), as required for the preconcentration step.

2.1.3. Chemical separation with TCF

It has been shown that TCF quantitatively adsorbs elements such as Se, Te, As, and Sb, depending on their various oxidation states (Yu et al., 1983). The major advantages for using this separation method before the determination of Se isotopes by HG-MC-ICP-MS are as follows. (1) The affinity of TCF for Se is very high, allowing us to achieve full yields of Se and to avoid any possible mass fractionation during chemical separation. (2) Removal of matrix-interfering elements for HG, such as transitional metals, is possible. (3) Quantitative separation of other hydride-forming elements, such as Sb, Ge, and As, occurs. The chemical separation of Se used in this study follows procedures described earlier (Yu et al., 1983; Xiao-Quan and Kai-Jing, 1985), although modifications have been made to improve the technique for use in isotope composition determination.

After the acid digestion and Se reduction, the solution in 4 N HCl is diluted to 1 N HCl, filtered through a 0.45-μm filter with a syringe, and then loaded onto 10-mL polypropylene columns. The columns are filled with 0.14 g of TCF previously washed with 3 mL H_2O and conditioned with 1 mL HCl 6 N and 1 mL HCl 1 N. Sb and residual matrix are eluted with 2 mL of HCl 6 N. Se is desorbed in bulk by impregnating the TCF placed in a 5-mL Pyrex tube (used once) with 100 μL of concentrated HNO_3 and 100 μL of H_2O. Complete desorbtion is obtained after partial attack of the cotton in a boiling-water bath for 20

min. The amount of nitric acid is an important parameter: amounts that are too low fail to desorb Se completely, and amounts that are too high create interference for the HG (signal suppression). A total of 3.3 mL of H_2O is then added to the tube before centrifugation to obtain a 0.4 N HNO_3 solution. Three milliliters of solution is then pipetted out and placed in polyethylene test tube with 0.5 mL of concentrated HCl.

2.2. Isotopic Measurements by HG-MC-ICP-MS

2.2.1. On-line HG apparatus

The HG system was built at the Centre de Recherches Pétrographiques et Géochimiques (CRPG) and is shown schematically in Figure 1. All the parameters for HG are listed in Table 1. For the gas–liquid separator, we used a modified Scott-type spray chamber cooled at 4°C without the nebulizer in place. A peristaltic pump was used to deliver the reducing agent and the sample to the HG system. After the gas–liquid separator and aerosol filter, the hydrides are transported via Teflon tubing ($\sim$3.2 mm inner diameter) directly to the ICP torch. Stability of the hydride formation was improved by the mixing coil (20 cm), consistent pumping of the liquid waste to the drain, and a second Ar inlet placed between the gas–liquid separator and the ICP-MS torch. The elimination of aerosol formed in the gas–liquid separator is also important to avoid a loss of sensitivity due to Na signal suppression from the reducing agent. The sample solution was drawn at an uptake rate of 0.2 mL min^{-1}.

Table 1. HG-MC-ICP-MS operating conditions.

Inductively coupled plasma	
RF power	1450 W
Plasma Ar flow rate	13 L min^{-1}
Intermediate Ar flow rate	1.1 L min^{-1}
Mass spectrometer	
Sample	Nickel
Skimmer	Nickel
Ar hexapole flow rate	1.8 mL min^{-1}
Data aquisition parameters	
Measurement time/sequence	8 s
Number of raw data	25
Hydride generation	
Reducing agent	1% (m/v) NaBH4 in 0.05% (m/v) NaOH
Flow rate of reducing agent	0.5 mL min^{-1}
Flow rate of sample	0.2 mL min^{-1}
Flow rate of carrier gas 1 (Ar)	0.9 L min^{-1}
Flow rate of carrier gas 2 (Ar)	0.2 L min^{-2}
Sample acidity HCl	1.7 N

Table 2. MERCK standard isotopic composition[a].

Isotope	MC-ICP-MS[b]	Relative deviation per mass unit (‰)	MC-ICP-MS[c]	Relative deviation per mass unit (‰)	N-TIMS[d]
$^{80}Se/^{74}Se$	57.15 ± 0.09	4.0 ± 1.6	55.99 ± 0.09	3.3 ± 2.3	55.80 ± 0.18
$^{80}Se/^{76}Se$	5.3689 ± 0.0024	3.4 ± 1.2	5.2970 ± —	0 ± —	5.2970 ± 0.0097
$^{80}Se/^{77}Se$	6.573 ± 0.010	3.8 ± 1.9	6.502 ± 0.010	0.6 ± 2.2	6.498 ± 0.008
$^{80}Se/^{78}Se$	2.1023 ± 0.0006	3.8 ± 1.3	2.0872 ± 0.0017	0.3 ± 1.2	2.0865 ± 0.0020
$^{80}Se/^{82}Se$	5.6498 ± 0.0011	2.9 ± 1.3	5.6896 ± 0.0066	1.3 ± 1.6	5.6823 ± 0.0065

[a] Values are expressed as ± standard error, based on 45 analytical runs.
[b] This study, $^{80}Se/^{82}Se$ ratio obtained after normalization with NBS 987 ($^{86}Sr/^{88}Sr$ = 0.1194). Analysis performed with Se/Sr between 0.5 and 2.
[c] This study, ratios obtained after normalization with $^{80}Se/^{76}Se$ ratio from Wachsmann and Heumann (1992).
[d] Wachsmann and Heumann (1992).

2.2.2. mc-icp-ms setting

A Micromass Isoprobe MC-ICP-MS operating at the CRPG has been used for the measurements of Se isotopes, and operating parameters are summarized in Table 1 and described below. The ions produced within the ICP source pass through the sample and skimmer cones and enter a Hexapole cell located behind the last skimmer cone. The ions are then concentrated into the center of the hexapole by the RF field and drawn into the transfer optics before entering the magnetic sector and analyzer system at 6-kV potential. By addition of small amounts of gases such as Ar at few a few milliliters per minute into the cell (typically 1.8 mL/min), the pressure in the Hexapole cell increases to approximately 0.0001 mbar, and subsequent collisions between the reactive gas and the ion beam reduce the energy spread of the ions from 20 to 30 eV to less than 1 eV. It has been shown that this "collisional focusing" (Douglas and French, 1992) in a RF-only hexapole device induces a series of ion–molecule reactions between the gas and the ion beam, allowing the removal of molecular ion interferences (Douglas, 1989; Eiden et al., 1996). For the determination of the major Se isotope, ^{80}Se suffering from a major Ar_2^+ interference, we used H_2 in addition to Ar (Ar/H = 4) as a collision gas to reduce the dimer of Ar to background levels <1 mV. The drawback of the use of H_2 in the hexapole collision cell is the formation of 1 to 4% of Se hydride SeH^+, which requires a correction for the accurate measurement of Se isotopes at masses 77 and 78. Thus, as explained below, only Ar is used as a collision gas for the routine analysis of isotopic composition of Se in natural samples. NiO^+ interferences coming from Ni cones at m/z 74 and 76 are significant and increase slightly at the background level but do not exceed the mV level. Kr, which may be present as an impurity in the Ar plasma gas, was found to be negligible at mass 82 and did not require specific correction. The isoprobe is equipped with an array of nine Faraday cups that permit the simultaneous measurement of all Se isotopes from mass 74 to 82.

2.2.3. Determination of SE isotope abundances

Selenium isotope abundances were determined in this study to intercalibrate with the measurements obtained by N-TIMS by Wachsmann and Heumann (1992). The procedure involves addition of a Sr-dopant to Se to correct for instrumental mass fractionation. A similar procedure was used for Cu and Zn measurement (Maréchal et al., 1999). Classical nebulization with a spray chamber and a mixture of Ar (1.5 mL min^{-1}) and H (0.3 mL min^{-1}) in the hexapole collision cell was used for the determination of Se isotope abundances of the internal standard MERCK. The ratio $^{86}Sr/^{88}Sr$ of certified isotopic standards NBS 987 ($^{86}Sr/^{88}Sr$ = 0.1194) was used to estimate the instrumental mass fractionation that is applied to correct the Se isotopic ratio $^{80}Se/^{82}Se$. The background was measured before each analysis by using the same solution used to dilute the standard solutions and subtracted from Se and Sr signal. The corrected $^{82}Se/^{80}Se$ ratio was used to calculate the relative isotopic abundances of other Se isotopes by using the internal normalization applied by Lee and Halliday (1995) for Mo, Te, Sn, and W. An exponential law was used to correct for mass discrimination. Se hydrides interferences at m/z 77 and 78 are corrected by evaluating the rate of hydride formation with the ratio $^{80}Se/^{80}SeH$ at m/z 80 and 81. Results are listed in Table 2 and are compared with previous determinations of Se natural abundance by N-TIMS (Wachsmann and Heumann, 1992). The difference in Se isotopic composition determined by the two methods corresponds, within the error, to a mass fractionation per mass unit of ~3.6‰. This discrepancy may be explained in part by the fact that Se and Sr instrumental mass bias may not be perfectly related when an exponential law is used, and also by the fact that Se and Sr might behave differently in the plasma and interface, so that the mass bias might be different. However, because replicate Se isotope measurements have been made over a period of more than 15 months with different instrumental settings and analytical procedures, the potential introduced mass bias is expected to be within the error estimate. As the results reported in this article are reported in delta notation; the uncertainty in the absolute Se isotopic composition of our standard MERCK does not affect the results. A second estimate of the Se isotope abundances is presented in Table 2 and has been obtained by normalizing our data to the Wachsmann and Heumann (1992) $^{80}Se/^{76}Se$ ratio. The difference in Se isotopic composition determined by the two methods is similar within the error.

2.2.4. Analysis of natural SE isotopic composition

Major Se isotopes are monitored during the analysis (i.e., ^{76}Se, ^{78}Se, ^{80}Se, and ^{82}Se) as well as Ge measured at mass 73. By using H in addition to Ar in the collision cell, it was found that the AsH contribution at mass 76 is not negligible for samples containing a ratio As/Se > 0.5. To obtain accurate measurement of the isotopic ratio $^{82}Se/^{76}Se$, we used only Ar as a collision gas. This also allows the measurement of the isotopic ratios $^{82}Se/^{78}Se$ and $^{82}Se/^{77}Se$ but not $^{80}Se/^{76}Se$, which suffers from major Ar_2 interferences.

The isotopic results are reported in the same manner as proposed for Fe and Cu isotope measurements by MC-ICP-MS (Belshaw et al., 2000; Zhu et al., 2000). This method involves the measurements of a standard (hereafter referred to as "matching standard") between samples yielding the isotopic composition of the sample expressed as a deviation relative to the standard following the equation

$$\delta^{82/76}Se = 1000 \times \left(\frac{R_{spl}}{R_{std}} - 1 \right) \quad (1)$$

where R_{spl} is the measured $^{82}Se/^{76}Se$ ratio (or other Se isotope couples) for the unknown sample and R_{std} is the mean $^{82}Se/^{76}Se$ ratio of the matching standard MERCK measured before and after the sample. Each data point given in this study corresponds to the mean of two or three replicate measurements of individual bracketed samples.

Measurements were made with an autosampler, including, generally, 14 samples and three standard solutions. The background was measured at the beginning of each run with a blank solution and subtracted from the Se mass spectra of both samples and the matching standard analysis. By use of this blank substration, we found that by keeping the standard and the sample at the same concentration within 30% difference, the interfering signal from NiO^+ (<1 mV) and minor Ar_2 (~1 mV) at mass 76 introduced no bias. The internal precision of the measurement of the samples is evaluated by the measurement of the standard solutions treated in the same way as for an unknown sample. Ge contribution at mass 76 is calculated by ^{73}Ge isotope and the ratio

Table 3. Standard solution reproducibility.

Method	Standard	Se analyzed (ng)	$\delta^{82/76}Se$ (‰)	$\delta^{82/77}Se$ (‰)	$\delta^{82/76}Se$ (‰)
HG-MC-ICP-MS	MERCK	8–200	0.01 ± 0.24 (61)	0.04 ± 0.32 (61)	0.01 ± 0.21 (61)
NEB-MC-ICP-MS	MERCK	750–3000	−0.05 ± 0.19 (16)	−0.06 ± 0.16 (16)	−0.05 ± 0.13 (16)
HG-MC-ICP-MS	CRPG	15–40	−3.15 ± 0.19 (4)	−2.59 ± 0.45 (4)	−2.13 ± 0.15 (4)
NEB-MC-ICP-MS	CRPG	1500–4000	−3.23 ± 0.27 (10)	−2.74 ± 0.38 (10)	−2.16 ± 0.18 (10)

$^{76}Ge/^{73}Ge$ corrected for instrumental mass fractionation. For each measurement of background, samples or matching standard, one block of 25 cycles of 8 s are measured and no data rejection is allowed. The Se isotopic composition of the sample is calculated at the end of the run after correction for background and Ge interference. A minimum of 2 mL of sample solution is analyzed at a concentration ranging from 5 to 50 ppb, generating a total Se signal between 0.5 to 5 V, respectively. The minimum Se required for the determination of $^{76}Se/^{82}Se$ ratios is 10 ng, but routine analyses were performed with 50 ng Se or more.

3. RESULTS AND DISCUSSION

3.1. Optimization of HG Conditions

The normality of HCl in the range of 1 to 4 N was not critical to the HG efficiency, but a concentration of 1.7 N was chosen to reduce the acid blank and to obtain a less vigorous reaction between the reductant and the sample solution, thus decreasing the formation of aerosols and increasing the stability of the signal. A concentration of $NaBH_4$ at 1% was adopted as reported for HG operating in continuous flow mode (Dedina and Tsalev, 1995). Memory effects in the glass HG system are not significantly higher than those observed for nebulization of the analyte in 0.05 N HNO_3. The washout time needed to decrease the signal below 1% of the previous sample is of the order of 150 s, which is acceptable for isotopic measurement. This memory is, however, carefully monitored to avoid any effect for samples with large differences in Se isotopic composition relative to the matching standard. The HG system, when compared with classic nebulization with spray chamber, results in an increase in sensitivity by a factor of 100. The instrumental mass fractionation per mass unit for Se is ~3.1% by either spray chamber or HG.

3.2. Interfering Elements and Chemistry Blank

It has been shown by Dedina and Tsalev (1995) that Se HG is strongly suppressed by transitional and heavy metals. After enrichment with TCF, these interferences are completely eliminated. Interferences between hydride-forming elements such as Ge (^{74}Ge and ^{76}Ge isotopes are isobaric interferences with Se isotopes) and potentially As (AsH^+ interferences at m/z 76) are important because these elements can be enriched by one or two orders of magnitude compared with Se in geological and biologic samples. It has been observed that between 2.8 and 3.4% of the original As content in a sample may remain in solution after the chemical separation. This suggests that under the analytical conditions, As, presumably present as As(V) species, has a slight affinity for TCF. However, with only Ar in the collision cell, there is no significant contribution of AsH on mass 76, and thus the $^{82}Se/^{76}Se$ ratio may be measured accurately. In contrast to As, Ge can easily be removed from Se after careful washing of the TCF column. We found that less

than 0.001% of the original Ge content in a sample is likely to be retained on TCF. However, Ge contribution from blank between the sample processed through chemistry and the matching standard may be different. Ge correction at mass 76 is therefore applied for each measurement to increase the accuracy of the $^{82}Se/^{76}Se$ ratio. After washing the TCF column with 2 mL of HCl 6 N, Sb is eluted, and less than 1% of the original Sb content is retained on TCF. As observed by Yu et al. (1983), the affinity of TCF for Te is very high, thus precluding the separation of Se from Te. In our experiments, between 90 and 100% of Te may remain in solution after chemical separation. However, because the Te concentrations in natural samples are often one or two orders of magnitude lower than those of Se, and because no matrix effects have been observed for the Se isotope standard composition that was doped with Te at a ratio of Te/Se equal to unity (see section 3.4), separation of Se from Te is not required. The contribution of Se from the whole procedural chemistry blank was measured for each batch of samples ($n = 12$) and has been found to be less than 100 pg and negligible. Furthermore, the isotopic composition of the Se from blank falls within the range of common Se isotopic composition and does not require any specific correction.

3.3. Analysis of Standard Solutions: Internal Reproducibility

To investigate the long-term internal reproducibility of our Se isotope ratio measurements as well as the precision and accuracy of the measurements that used HG, we performed replicate measurements of our internal standard MERCK during a 24-month period; we used classic nebulization and HG for sample injection (Table 3). Two other Se standard solutions, CRPG, prepared from Se metal pellets, and MH495, obtained from T. Johnson and used in Johnson et al. (1999), have also been measured relative to the MERCK internal standard, and the results are presented in Tables 3 and 4. We estimate our present internal precision at 0.25‰ (95% confidence level) for the working $^{82}Se/^{76}Se$ ratio. The quantity of Se used per analysis is reported in Figure 2 and compared with the minimum amount required by other techniques, as reported by Johnson et al. (1999) and Krouse and Thode (1962). Because of the high sensitivity of HG-MC-ICP-MS, the analytical procedure decreases by one order of magnitude the minimum Se amount required per analysis when compared with the N-TIMS method. The precision obtained via the "bracketing" technique has a similar analytical uncertainty for the ratio $^{82}Se/^{76}Se$ when compared with double-spike method.

Table 4. Standards processed through TCF.

Standard	Se analyzed (ng)	$\delta^{82/78}Se$ (‰)	$\delta^{82/77}Se$ (‰)	$\delta^{82/78}Se$ (‰)
MH495 (unprocessed)	50	−4.46	−3.82	−3.06
MH495	50	−4.67	−3.86	−3.02
CRPG (unprocessed)	15–40	−3.15	−2.59	−2.13
CRPG	50	−3.46	ND[a]	−2.20
CRPG	100	−3.33	−2.86	−2.12
MERCK	25	0.12	ND	−0.11
MERCK	50	−0.17	ND	0.15
MERCK	100	0.20	0.05	0.13
MERCK	150	−0.14	−0.22	−0.18
MERCK	500	0.13	0.14	0.07
MERCK[b]	500	0.23	0.08	0.15
MERCK[b]	400	0.15	0.13	0.11
MERCK[b]	200	0.15	0.02	0.07
MERCK[b]	100	0.10	−0.08	−0.03
MERCK[b]	50	0.27	0.23	0.24
MERCK[b]	25	0.28	0.14	0.11
MERCK[c]	50	−0.09	−0.07	−0.06
MERCK[c]	50	0.15	0.26	0.02
MERCK[c]	40	0.19	0.12	0.21
MERCK[b,c]	50	0.05	0.14	0.21
MERCK mean		0.12	0.07	0.07
2 standard deviations		0.25	0.27	0.25

[a] ND = not determined.

[b] MERCK standard solution doped with basalt matrix (500 mg) and processed through TCF.

[c] MERCK standard solution doped with As, Sb, Ge, and Te (As/Se=50, Sb/Se = 1, Te/Se = 1, and Ge/Se = 10) and processed through TCF.

3.4. Analytical Accuracy: External Reproducibility

The procedure adopted here for the measurement of Se isotope ratios has been evaluated by the replicate measurements of standard solutions (MERCK, CRPG, or MH495) processed through the complete chemical preparation. Furthermore, prior the chemical purification, the standard solution (MERCK) was doped with other hydride-forming elements (As, Ge, Sb, and Te) and geological matrix prepared as described in Marin et al. (2001). The results are presented in Table 4, and for all samples
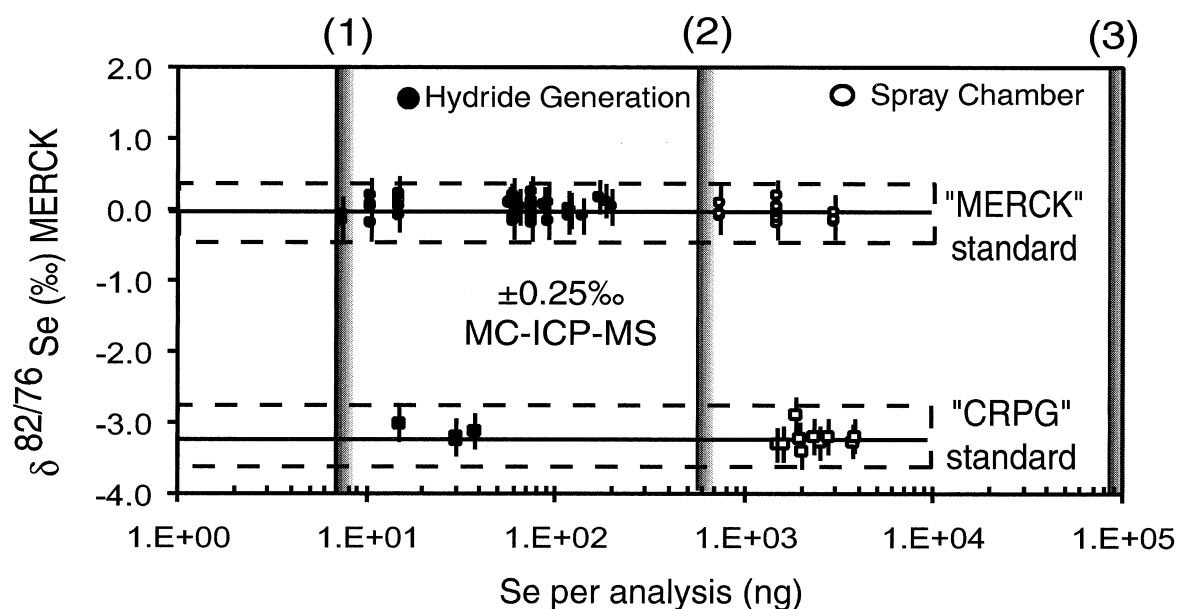

Fig. 2. Plot of $\delta^{82/76}Se$ vs. the quantity of Se used per analysis (ng). The precision of the use of either HG or the spay chamber for two internal standards (MERCK and CRPG) is evaluated at 0.25‰ (2 standard deviation). The limits of determination of different methods are shown (1) 5 ng: HG coupled to MC-ICP-MS (this study); (2) 500 ng: double spike N-TIMS (Johnson et al., 1999); (3) ∼100 μg: gas source mass spectrometer (Krouse and Thode, 1962).

Table 5. Se isotopic composition of geochemical reference materials.

Sample	Sample type	As/Se	Ge/Se	Se (ppm)	Se analyzed (ng)	$\delta^{82/76}Se$	$\delta^{82/77}Se$	$\delta^{82/78}Se$
MAG-1	Marine mud	7.9	ND[a]	1.16	250	−1.42	−1.24	−0.76
					250	−1.33	−1.27	−0.88
NIST-2711	Montana Soil	69.1	ND	1.52	250	−1.75	−1.07	−0.91
					250	−1.97	−1.35	−1.23
BCR 176	Waste	ND	ND	42.70	50	−3.15	−2.75	−1.99
					50	−2.98	−2.55	−2.08
GSD-3	Stream sediment	16.6	1.2	1.06	250	−1.74	−1.40	−0.94
GXR-1	Jasperoid	25.7	ND	16.60	250	−0.73	−0.47	−0.49
					250	−0.96	ND	−0.64
GXR-5	Soil	10	ND	1.12	250	−2.81	−2.28	−1.76
SCo-1	Shale (Cody shale)	13.9	1.1	0.89	250	−1.57	−1.24	−0.92
					250	−1.48	−1.02	−0.79
SGR-1	Shale	19.1	0.5	3.50	250	−1.08	−0.95	−0.68
BCR-1	Basalt	7.4	17	0.09	50	−1.30	−1.35	−0.73
BR	Basalt	32.3	19.4	0.06	50	−1.04	−0.95	−0.86
					50	−1.12	−0.90	−0.69
					50	−1.22	−0.97	−0.71
BE-N	Basalt	31.6	21.1	0.057	50	−1.17	−0.72	−0.48
BHVO-1	Basalt	5.4	22.2	0.074	25	−1.22	−0.98	−0.70
GXR-4	Copper mill-head	17.5	ND	5.6	50	−1.29	−1.24	−0.88
PCC-1	Peridotite	2.1	34.8	0.027	25	−1.30	ND	−0.88
DR-N	Diorite	36.6	23.2	0.082	50	−2.09	−1.70	−1.36
GSR-6	Limestone	47.5	6.8	0.099	50	−1.11	−0.99	−0.60
GSR-4	Sandstone	92.9	11.8	0.098	50	−1.60	−1.52	−1.18
GSR-5	Shale	16.7	36.9	0.084	50	−0.92	−0.57	−0.58
IF-G	Iron formation	17	273	0.088	50	−0.17	0.01	0.06
						−0.37	n.d	−0.11
NOD-P-1	Mn nodule	ND	ND	0.5[b]	200	−1.12	−0.85	−0.69
						−1.23	−0.86	−0.73

[a] ND = not determined.
[b] Indicative value.

presented, the yield of the chemical purification ranges between 95 to 100%. The isotopic results of the standard processed through chemistry compared with unprocessed standards suggest that, within error, there is no isotopic fractionation during sample purification. Furthermore, because Se desorption from TCF is performed in batch, no chromatographic fractionation of Se isotopes is expected in contrast to stepwise elution.

The overall external analytical precision for the ratios $^{82}Se/^{76}Se$, $^{82}Se/^{78}Se$, and $^{82}Se/^{77}Se$ is estimated to be 0.25‰ (95% confidence level). This precision is confirmed with the duplicate measurements of natural samples presented below.

3.5. Selenium Isotopic Composition of Natural Samples

Several geochemical reference materials have been analyzed for their Se isotopic composition (Table 5). These samples cover a large range of Se concentrations (from 40 ppb to 10 ppm) and have different matrices and As/Se and Ge/Se ratios. Replicate measurements of natural samples are consistent and yield a precision of 0.25‰ for the $^{82}Se/^{76}Se$ ratio for all geological materials having a concentration as low as 25 ppb. All the samples (Tables 5 and 6) fall within the error along the theoretical mass fractionation line (Fig. 3), suggesting that Se isotopic composition can be measured by HG-MC-ICP-MS at the nanogram level without interference.

3.5.1. Meteorites and igneous mantle rocks

To identify the bulk Earth Se isotopic compositions, we analyzed terrestrial igneous mantle rocks and meteorites (Ta-

bles 5 and 6). As already observed for S isotopes, it seems that the mantle and meteorites Se isotopic variations are limited to a small range of less than 0.5‰. Furthermore, iron meteorites do not deviate, within error, from the isotopic composition of the Earth. However, further investigations of possible mass-dependent and/or isotopic anomalies of Se isotopes in chondrites are required to test if the solar nebular material was homogeneous with respect to Se. We are conducting studies of
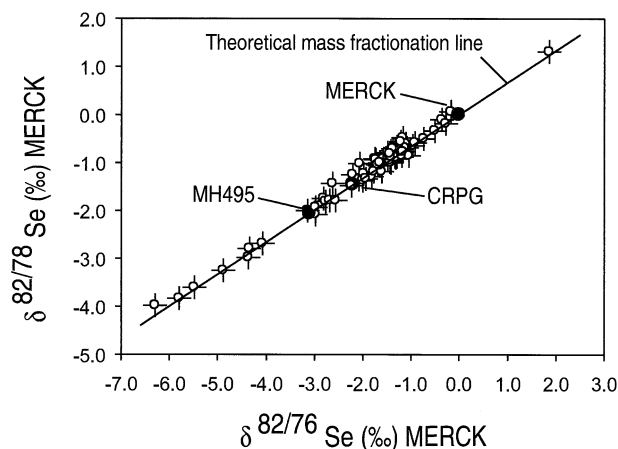

Fig. 3. Correlation of $\delta^{82/78}Se$ and $\delta^{82/76}Se$ for a suite of samples and standard solutions (MERCK, CRPG, MH495). The theoretical relationship between the ratios is given by the solid line (on the basis of a linear fractionation).
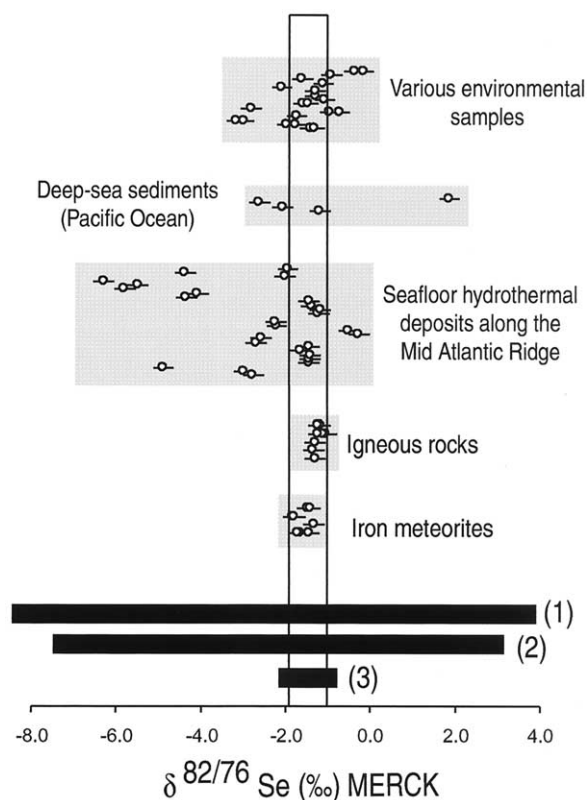
Fig. 4. Diagram showing the distribution of $\delta^{82/76}$Se in a selection of iron meteorites, igneous rocks, sediments, and hydrothermal sulfides. Results are expressed as per mil deviation relative to the internal standard MERCK. Light gray boxes represent the range of isotopic composition for each sample type. The open box represents the bulk Earth isotopic composition estimated from the composition of igneous rocks and iron meteorites. Black boxes represent the range of Se isotope fractionation (1) obtained during chemical partial reduction of Se oxyanions (Se(IV) and Se(VI)) to elemental Se (Krouse and Thode, 1962; Rees and Thode, 1966; Johnson et al., 1999); (2) observed during bacterial respiratory reduction of selenium oxyanions (Herbel et al., 2000); (3) observed from soil-Se oxidation and soil-Se volatilization experiments (Johnson et al., 1999).

acid-leached carbonaceous chondrites with the measurement of the six Se isotopes to address this issue. Morgan (1986) and Yi et al. (2000) have suggested that the entire budget of Se, as well as S and Te, in the silicate Earth was added by the late veneer. Therefore, it seems to be promising to investigate the cosmochemistry of Se coupled with Te to test if any relationship can be drawn between the Earth's mantle and the extraterrestrial material that may have bombarded the Earth in its late accretionary stages.

3.5.2. Marine sediments and hydrothermal deposits

We performed preliminary Se isotope ratio measurements of marine sediments and seafloor hydrothermal deposits to investigate possible Se isotope fractionation in natural environments where complex processes such as redox changes, rock/seawater interaction, and biologic activity may occur. Both Se-rich sulfides (up to 1600 ppm) and depleted siliceous deep-sea sediments (down to 0.05 ppm) have been analyzed, and an overall Se isotope range of 8.0‰ has been obtained (Fig. 4). In contrast

to the constant Se isotope composition of igneous rocks, the isotopic compositions of Se in sedimentary or hydrothermal environments are highly variable.

These results suggest that the observed variability is related to abiotic or bacterial processes at low temperature. Seawater mixing may also explain part of the variations observed, but the Se isotopic composition of seawater must be defined to further elucidate such an effect. Se exists in deep-sea water as Se(IV) and Se(VI) oxyanions, and among other characteristics, these two valences have a distinctly different behavior with respect to adsorption onto particles. The relative proportion of each species varies with ocean depth, oxygen fugacity, and biologic productivity (Cutter and Bruland, 1984). To date, to our knowledge, no isotopic composition of these species in seawater has been reported, mainly as a result of the low concentration of Se in seawater below 1.7×10^{-9} mol/L. The sensitivity of this analytical procedure will likely permit the determination of Se isotopic composition of seawater but requires further development for the selective enrichment of Se(VI) species in seawater. However, as Se oxyanions in seawater are scavenged in marine ferromanganese concretions (Takematsu et al., 1990), we suggest that Se isotopic composition of Mn nodules may approximate the isotopic composition of seawater. On the basis of the isotopic composition of a Mn nodule (sample NOD-A-1, Table 5), which has an isotopic value at −1.5‰, there is no evidence that seawater is greatly fractionated relative to the bulk Earth value, as might be expected if one assumes that the marine Se cycle is similar to the marine sulfur cycle. The large range and highly negative values of hydrothermal deposits observed, in particular at Lucky Strike hydrothermal field and Menez Gwen (Table 6), cannot be explained by simple mixing between Se leached from igneous rock and Se derived from seawater. Previous investigation of Johnson et al. (1999) reported measurements of Se isotope fractionation during selenate reduction, selenite sorption, and oxidation of reduced Se. These results, combined with previous studies performed by Rashid and Krouse (1985), indicate that reduction of soluble oxyanions is the major source of Se isotope fractionation. Therefore, on the basis of current knowledge of Se isotope fractionation, we conclude that partial reduction of Se oxyanions (selenate and selenite) must occur in these systems. We are undertaking studies to evaluate whether bacterial or abiotic partial reduction of Se is the likely cause of Se isotope fractionation in hydrothermal systems (Rouxel et al., 2001). One of the most promising tests is the comparison of Se isotopes with more commonly used stable isotopes such as S, which may be used to quantify the extent of seawater S (and Se) oxyanion reduction (i.e., partial reduction or quantitative reduction).

4. CONCLUSIONS

In this study, we presented a method for the sensitive and precise determination of Se isotopes by MC-ICP-MS by use of an on-line HG system for sample introduction. Instrumental mass bias is easily corrected by the "standard-sample bracketing" method. Important advantages of the use of HG-MC-ICP-MS for the determination of Se isotopes relative to the other alternative method—that is, double-spike N-TIMS are high sensitivity, lowering the total amount of Se required for one analysis down to 10 ng (compared with 500 ng by N-

Table 6. Se isotopic composition of selected samples[a].

Sample	Sample type	Se (ppm)	$\delta^{82/76}Se$	$\delta^{82/78}Se$
Meteorites				
Bella Roca	Iron meteorite (troilite phase)	100[b]	−1.45	−0.97
			−1.65	−1.06
			−1.69	−1.05
Canon Diablo troilite	Iron meteorite (troilite phase, partly oxidized)	10[b]	−1.32	−0.89
Canon Diablo troilite[c]			−1.10[c]	
Not sure about twhat this should be here				
Gibeon	Iron meteorite (troilite phase)	50[b]	−1.82	−1.29
			−1.76	−1.19
Nantan	Iron meteorite (bulk sample)	5[b]	−1.48	−0.91
			−1.42	−1.00
Marine sediments				
1149A-10H3,140	Deep-sea sediment, ash-bearing siliceous clay	0.05	−1.19	−0.86
1149A-1H1,140	Deep-sea sediment, ash- and silica-bearing clay	0.13	−2.07	−1.02
1149A-4H2,140	Deep-sea sediment, ash-bearing siliceous clay	0.06	−2.62	−1.43
1149B-29R2,7	Deep-sea sediment, Mn rich and carbonate rich, sampled near the basement contact	0.22	1.86	1.31
Menez Gwen hydrothermal field				
DV-14-06 altB	Hydrothermally altered basalt (slab) at Menez Gwen field	60.30	−2.76	−1.82
DV-16-03 altB	Hydrothermally altered basalt (slab) at Menez Gwen field	59.70	−2.98	−1.94
DV-16-03 py	Hand-picked sulfides (marcasite) from slab	25.60	−4.88	−3.25
Lucky Strike hydrothermal field				
DV-1-2 basalte	Basaltic glass from a lava lake at Lucky Strike field	0.17	−1.29	−0.66
DV-6-2 basalte	Vesicular lava around the Lucky Strike field	0.07	−1.34	−0.70
FL-DR py	Hand-picked sulfide (pyrite) from massive sulfides	2	−1.22	−0.57
			−1.18	−0.78
FL-DR cpy	Hand-picked sulfide (chalcopyrite) from massive sulfides	1488	−1.38	−0.71
			−1.44	−0.96
FL-19-08 py/mar	Massive pyrite and marcasite aggregate from low-temperature active vent	10	−4.34	−2.79
			−4.07	−2.68
FL-20-04a cpy	Chalcopyrite lining central conduit of active high-temperature black smoker Same (resampled)	215	−5.79	−3.83
			−5.49	−3.60
	Same (resampled)		−6.29	−3.97
ALV-2605-3-1 py	Massive marcasite intergrowth with barite from diffuse vent	1	−2.01	−1.37
ALV-2608-2-1 cpy	Euhedral to anhedral chalcopyrite filling central chimney conduit	315	−4.37	−2.98
FL-19-05 py	Porous zone of chimney composed of massive to finegrained pyrite with marcasite	27	−1.94	−1.33
Rainbow hydrothermal field				
FL-07-01 serp	Serpentinite from the Rainbow field	0.48	−1.44	−0.82
FL-10-07 cpy	Isocubanite lining central conduit of active high-temperature black smoker	1315	−2.69	−1.79
FL-10-07 bn-cv	Alteration rim (bornite–covellite) of high-temperature black smoker	460	−2.57	−1.80
FL-07-09 sph	Sphalerite lining central conduit of inactive chimney	1	−0.27	−0.18
			−0.51	−0.34
FL-06-08 cpy	Chalcopyrite lining central conduit of active high-temperature black smoker	1625	−2.21	−1.25
			−2.23	−1.48
Logatchev hydrothermal field				
MS-21-08-2/2A bncv	Alteration rim (bornite, covellite) of Cu-rich chimney	1220	−1.43	−0.87
MS-21-08-2/2C cpy	Chalcopyrite from chimney wall of active high-temperature black smoker	1590	−1.41	−0.88
MS-21-08-2/2D cpy	Chalcopyrite from chimney wall of active high-temperature black smoker	1410	−1.65	−1.01
MS-21-08-2/2E cpy	Chalcopyrite lining central conduit of active high-temperature black smoker	1500	−1.44	−0.82

[a] Marine sediments have been collected during the ODP cruise, leg 185. Samples from Menez Gwen, Lucky strike, Rainbow, and Logatchev hydrothermal fields have been sampled along the mid-Atlantic Ridge during the DIVA1, FLORES, and MICROSMOKE cruises.
[b] Indicative values.
[c] Isotopic composition calculated with $\delta^{80/76}Se = 2.3‰$ relative to MH495 (T. Johnson, personal communication.)

TIMS); and they permit simultaneous determination of all the six Se isotopes, allowing the study of potential isotopic anomalies in meteorites. The external precision obtained for the $^{82}Se/^{76}Se$ ratio is 0.25‰ at 95% confidence level and allows identification of natural variations of Se isotopes. Although the HG system is by itself a method to isolate Se from the geological matrix, a preconcentration step is required for accurate analysis. The preconcentration step removes not only metals causing Se HG suppression, but also Ge, which has an isobaric interference. Arsenic, which can be enriched by a factor of 100 relative to Se and can be a source of AsH interference for Se analysis, does not interfere with Se isotope measurements after partial separation with TCF and the use of only Ar in the collision cell of the ICP-MS.

Terrestrial igneous rocks and iron meteorites have been analyzed for their Se isotopic composition, allowing us to define a bulk Earth reservoir. Se deposited in sedimentary and hydrothermal environments has a significant range of Se isotopic composition (up to 8‰), which confirms the early experimental and theoretical studies of Krouse and Thode (1962). These variations may reflect not only different Se source contribution but also mass dependent, kinetic fractionation occurring at low temperature in aqueous media. Because Se is a trace element in most natural systems (below 0.1 ppm) but is readily concentrated biologically as an essential nutrient, Se isotopes are expected to be an ideal geochemical fingerprint to identify biologic activity in modern environments (such as seafloor hydrothermal systems) and, probably, ancient environments. Se isotopes are known to be fractionated to the same extent during both biotic and abiotic processes. Therefore, only a multitracer approach that uses, for example, S and Se isotopes may allow differentiation of the effects of biologic from abiotic processes.

Associate editor: K. Kyser

REFERENCES

Belshaw N. S., Zhu X. K., Guo Y., and O'Nions R. K. (2000) High precision measurement of iron isotopes by plasma source mass spectrometry. *Int. J. Mass Spectrom. Ion Processes* **197,** 191–195.

Brimmer S. P., Fawcett W. R., and Kulhavy K. A. (1987) Quantitative reduction of selenate ion to selenite in aqueous samples. *Anal. Chem.* **59,** 1470–1471.

Cutter G. A. and Bruland K. W. (1984) The marine biogeochemistry of selenium: A re-evaluation. *Limnol. Oceanogr.* **6,** 1179–1192.

Dedina J., Tsalev D. L. (1995) *Hydride Generation Atomic Absorption Spectrometry.* Wiley.

Douglas D. J. (1989) Some current perspectives on ICP-MS. *Can. J. Spectrosc.* **2,** 38–49.

Douglas D. J. and French J. B. (1992) Collisional focusing effects in radio frequency quadripoles. *J. Am. Soc. Mass Spectometr.* **3,** 398–408.

Eiden G. C., Barinaga C. J., and Koppenaal D. W. (1996) Selective removal of plasma matrix ions in plasma source mass spectrometry. *J. Anal. Atom. Spectrom.* **11,** 317–322.

Frankenberger W. T., Benson S. (1994) *Selenium in the Environment.* Marcel Dekker.

Halliday A. N., Lee D.-C., Christensen J. N., Walder A. J., Freedman P. A., Jones C. E., Hall C. M., Yi W., and Teagle D. (1995) Recent developments in inductively coupled plasma magnetic sector multiple collector mass spectrometry. *Int. J. Mass Spectrom. Ion Processes* **146/147,** 21–33.

Herbel M. J., Johnson T. M., Oremland R. S., and Bullen T. D. (2000) Fractionation of selenium isotopes during bacterial respiratory reduction of selenium oxyanions. *Geochim. Cosmochim. Acta* **64,** 3701–3709.

Johnson T. M., Herbel M. J., Bullen T. D., and Zawislanski P. T. (1999) Selenium isotope ratios as indicators of selenium sources and oxyanion reduction. *Geochim. Cosmochim. Acta* **63,** 2775–2783.

Krouse H. R. and Thode H. G. (1962) Thermodynamic properties and geochemistry of isotopic compounds of selenium. *Can. J. Chem.* **40,** 367–375.

Lee D.-C. and Halliday A. N. (1995) Precise determinations of the isotopic compositions and atomic weights of molybdenum, tellurium, tin and tungsten using ICP magnetic sector multiple collector mass spectrometry. *Int. J. Mass Spectrom. Ion Processes* **146/147,** 35–46.

Maréchal C. D., Télouk P., and Albarède F. (1999) Precise analysis of copper and zinc isotopic compositions by plasma-source mass spectrometry. *Chem. Geol.* **156,** 251–273.

Marin L., Lhomme J., Carignan J. (2001) Determination of selenium concentration in sixty five reference materials for geochemical analysis by GFAAS after separation with thiol cotton. Geostandard Newslett., **25,** 317–324.

Morgan J. W. (1986) Ultramafic xenoliths: Clues to Earth's late accretionary history. *J. Geophys. Res.* **91,** 12375–12387.

Rashid K., Krouse H. R., and McCready R. G. L. (1978) Selenium isotope fractionation during bacterial selenite reduction. *Short Papers of the Fourth International Conference, Geochronology, Cosmochronology, Isotope Geology.* In: (ed. R. E. Zartman). Geological Survey, U.S, 347–348.

Rashid K. and Krouse H. R. (1985) Selenium isotopic fractionation during SeO_3^{2-} reduction to Se ^{0} and H_2Se. *Can. J. Chem.* **63,** 3195–3199.

Rees C. E. and Thode H. G. (1966) Selenium isotope effects in the reduction of sodium selenite and of sodium selenate. *Can. J. Chem.* **44,** 419–427.

Rouxel O., Fouquet Y., Ludden J. (2001) Copper, selenium and sulphur isotope systematics of seafloor hydrothermal systems. EUG XI Meeting. *J. Conf. Abs.* **6,** 689.

Takematsu N., Sato Y., Okabe S., and Usui A. (1990) Uptake of selenium and other oxyanionic elements in marine ferromanganese concretions of different origins. *Mar. Chem.* **31,** 271–283.

Turner P. J., Mills D. J., Schröder E., Lapitajas G., Jung. G., Iacone L. A., Haydar D. A., Montaser A. (1998) Instrumentation for low- and high-resolution ICP-MS. In *Inductively Coupled Plasma Mass Spectrometry* (ed. A. Montaser), pp. 421–501. Wiley-VCH.

Wachsmann M. and Heumann K. G. (1992) Negative thermal ionization mass spectrometry of main group elements Part 2. 6th group: Sulfur, selenium and tellurium. *Int. J. Mass Spectrom. Ion Processes* **114,** 209–220.

Xiao-Quan S. and Kai-Jing H. (1985) Matrix modification for determination of selenium in geological samples by graphite-furnace atomic-absorption spectrometry after preseparation with thiol cotton fibre. *Talanta* **32,** 23–26.

Yi W., Halliday A. N., Alt J. C., Lee D. C., Rehkämper M., Garcia M. O., and Su Y. (2000) Cadmium, indium, tin, tellurium, and sulfur in oceanic basalts: Implications for chalcophile element fractionation in the Earth. *J. Geophys. Res.* **105,** 18927–18948D.

Yu M.-Q., Liu G.-Q., and Jin Q. (1983) Determination of trace arsenic, antimony, selenium and tellurium in various oxidation states in water by hydride generation and atomic-absorption spectrophotometry after enrichment and separation with thiol cotton. *Talanta* **30,** 265–270.

Zhu X. K., O'Nions R. K., Guo Y., Belshaw N. S., and Rickard D. (2000) Determination of natural Cu-isotope variation by plasma-source mass spectrometry: Implications for use as geochemical tracers. *Chem. Geol.* **163,** 139–149.